Improving mass detection performance by use of 3D difference filter in a whole breast ultrasonography screening system

Yuji Ikedo[a], Daisuke Fukuoka[b], Takeshi Hara[a], Hiroshi Fujita[a],
Etsuo Takada[c], Tokiko Endo[d], and Takako Morita[e]

[a]Department of Intelligent Image Information, Graduate School of Medicine, Gifu University,
1-1 Yanagido, Gifu-shi, Gifu 501-1194, Japan;
[b]Technology Education, Faculty of Education, Gifu University,
1-1 Yanagido, Gifu-shi, Gifu 501-1193, Japan;
[c]Center of Medical Ultrasonics, Dokkyo Medical University School of Medicine,
880 Kitakobayashi, Mibu-cho, Shimotsuga-gun, Tochigi 321-0293, Japan;
[d]Department of Radiology, National Hospital Organization Nagoya Medical Center,
4-1-1 Sannomaru, Naka-ku, Naogya-shi, Aichi 460-0001, Japan;
[e]Department of Mammary Gland, Chunichi Hospital,
3-6-38 Marunouchi, Naka-ku, Nagoya-shi, Aichi 460-0002, Japan

ABSTRACT

Ultrasonography is one of the most important methods for breast cancer screening in Japan. Several mechanical whole breast ultrasound (US) scanners have been developed for mass screening. We have reported a computer-aided detection (CAD) scheme for the detection of masses in whole breast US images. In this study, the method of detecting mass candidates and the method of reducing false positives (FPs) were improved in order to enhance the performance of this scheme. A 3D difference (3DD) filter was newly developed to extract low-intensity regions. The 3DD filter is defined as the difference of pixel values between the current pixel value and the mean pixel value of 17 neighboring pixels. Low-intensity regions were efficiently extracted by use of 3DD filter values, and FPs were reduced using a FP reduction method employing the rule-based technique and quadratic discriminant analysis with the filter values. The performance of our previous and improved CAD schemes indicated a sensitivity of 80.0% with 16.8 FPs and 9.5 FPs per breast, respectively. The FPs of the improved scheme were reduced by 44% as compared to the previous scheme. The 3DD filter was useful for the detection of masses in whole breast US images.

Keywords: computer-aided detection, whole breast ultrasonography, mass detection

1. INTRODUCTION

Since 1996, the first incident rate of breast cancer has been increasing in Japanese women. In order to detect and treat breast cancers at early stage are important for a better prognosis. Mammography is widely used as a principal method in breast cancer screening, however, it is less effective for younger women or women with dens breast tissues.[1,2] In addition, typically, Japanese women have denser breast tissues than their counterparts in Western countries. Ultrasonography can clearly depict masses, which are one of the important findings in interpreting breast cancers, in such dense breasts. Therefore, ultrasonography has been also used in Japan for breast cancer screening.

Some whole breast ultrasound (US) scanners have been developed for mass screening, such as SomoVu (U-Systems, Inc.)[3] and ASU-1004 (Aloka CO., LTD.).[4] By using these scanners, a large number of - several dozen or several hundred - image slices per breast are acquired, and their mass screening is expected to generate a large number of images. As a result, this is more likely to lead to oversight errors because of an increase in

corresponding author email: ikedo@fjt.info.gifu-u.ac.jp

Medical Imaging 2008: Computer-Aided Diagnosis, edited by Maryellen L. Giger, Nico Karssemeijer
Proc. of SPIE Vol. 6915, 691523, (2008) · 1605-7422/08/$18 · doi: 10.1117/12.769301

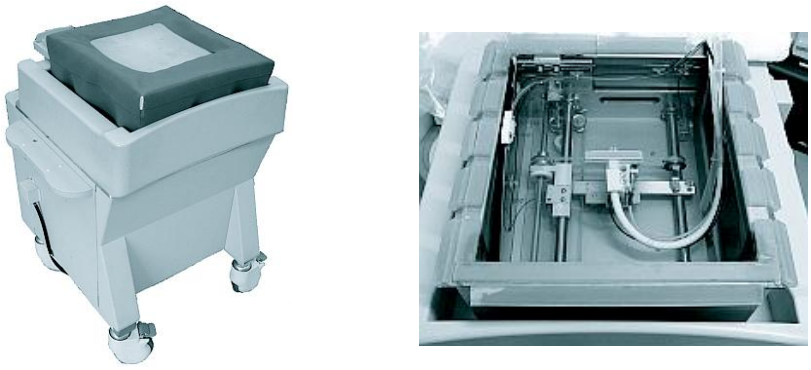

(a) (b)

Figure 1. The whole breast ultrasound scanner ASU-1004. (a) Appearance of the scanner. (b) Top view after removing the membrane.

the radiologist's workload in image interpretation. This possibility might be reduced by using computer-aided detection (CAD) systems. We have developed a CAD system for the detection of masses in whole breast US images.

Some breast ultrasonographic CAD schemes for detection of masses have been reported by several research groups. Drukker *et al.* reported an automatic lesion detection scheme that employs radial gradient index filtering.[5,6] Chang *et al.* proposed a mass detection method in whole breast US images that uses gray sclae thresholding.[7] Fukuoka *et al.* developed a CAD scheme based on an active contour model and an active balloon model in two-dimensional (2D) and three-dimensional (3D) spaces, respectively.[8] However, some studies were not based on whole breast images acquired by a whole breast US scanner and some proposed methods may be considered difficult for detecting the masses with posterior attenuation. Our proposed scheme uses two features of edge directions and intensity difference between slice images, and it was able to detect the masses with posterior attenuation.[9,10] Our previously reported CAD method was applied to a larger database than in the past, and it was found that the false positives (FPs) were remarkably increased. Therefore, in this study, the method of detecting mass candidates and the method of reducing FPs were improved in order to enhance the performance.

2. MATERIALS

2.1 Data acquisition

Whole breast US images were obtained by using a Prosound-II SSD-5500 US system with a whole breast US scanner ASU-1004 as shown in Figure 1, which are developed by Aloka CO., LTD., Japan. This scanner has a 6-cm linear transducer (probe) with a frequency range of 5-10 MHz, and the probe is immersed in a water tank where it moves mechanically. A special membrane is set on the tank, and a subject sets her breast on this membrane in a prone posture. An entire breast can be scanned with an area of 16×16 cm^2 in three overlapping runs. The interval between two images is 2 mm. A slice image of the whole breast is generated from the three original images by using our previously proposed image integration technique.[10]

2.2 Database

A whole breast image obtained after applying the image integration technique to the original images comprised 84 slice images with 2-mm intervals. Its width and height were 694 pixels and 400 pixels, respectively, with 256 gray levels. The database consisted of 260 breasts including 208 normal breasts and 52 abnormal breasts with 70 masses. The effective diameters of these masses were in the range of 5-20 mm. Figure 2 2 shows an example of a slice image of the whole breast with a mass. All cases were diagnosed by an experienced radiologist.

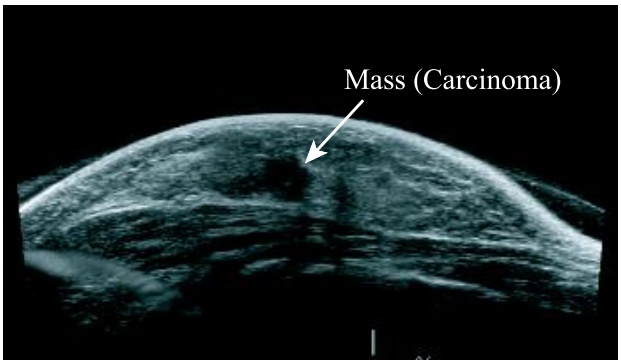

Figure 2. Example of a whole breast slice image with a mass.

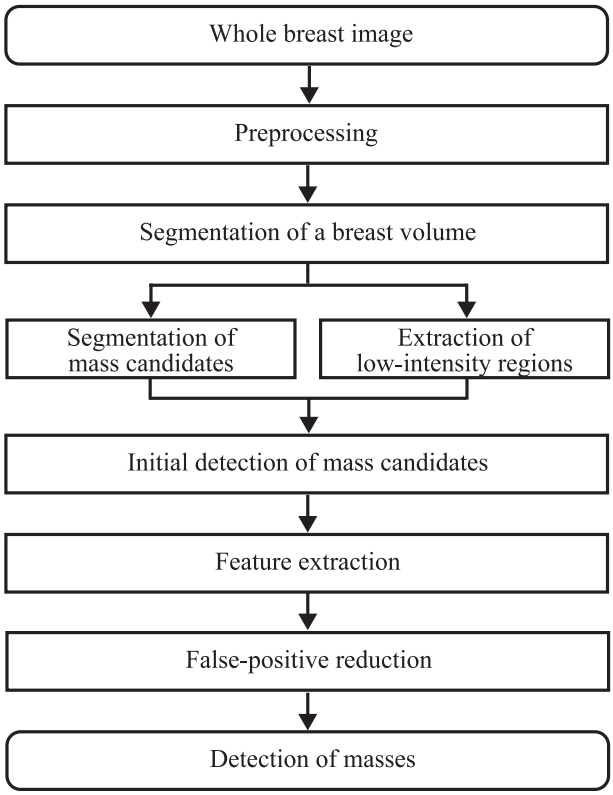

Figure 3. Overall CAD scheme for detection of masses in whole breast ultrasound images.

3. METHODS

3.1 Overall CAD scheme

The Overall CAD scheme for the detection of masses in whole breast US images consisted of seven steps as shown in Figure 3: (1) preprocessing, (2) segmentation of breast volume, (3) segmentation of mass candidates, (4) extraction of low-intensity regions, (5) initial detection of mass candidates, (6) feature extraction, (7) reduction of FPs, and finally annotation of the detected mass candidates.

US images always include a large amount of speckle noise, and the image brightness varies as we adjust the gain control of a US device. Therefore, in the first step, preprocessing, we removed the noise by use of a

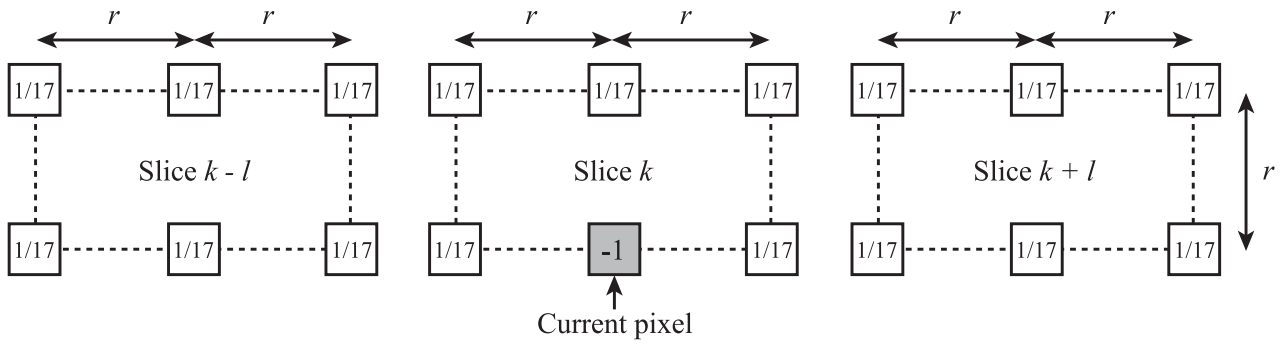

Figure 4. 3D difference (3DD) filter mask.

median filter and then an anisotropic diffusion filter;[11] then we normalized the brightness by using the employed gray-scale transformation.

In the second step, we segmented a breast volume from the background by use of gray-scale thresholding followed by the largest component selection.

In the third step, mass candidates were segmented by use of our previously proposed method.[10] First, mass candidates were identified using edge directions. Edge images of breast US images without a mass typically consist of near-horizontal edges only. However, edge images of breast US images with a mass include near-vertical edges. Therefore, these near-vertical edges were used as a cue to identify mass candidates and a location with two combinations of edges, i.e., two near-vertical edges or two near-vertical edges and a single near-horizontal edge, were determined as a mass candidate. In order to detect edges, we employed the Canny edge detector.[12] Finally, mass candidates were segmented from the parenchymal background by use of a watershed algorithm.[13,14]

In this study, we improved the remaining four steps. The previously proposed methods[10] are as follows. Generally, masses are depicted as hypoechoic regions. Therefore, low-intensity regions in US images were extracted using a slice subtraction method. If a mass candidate region segmented in the third step included a low-intensity region, the candidate region was detected as an initial mass candidate region. For each initial mass candidate region, the following five features were extracted: its are, average density, position of center of gravity, difference of average density and depth-to-width. In the final step, FPs were reduced employing two methods, namely, rule-based technique and quadratic discriminant analysis (QDA), which are described below.

3.2 Extraction of low-intensity regions

Difference of only two pixel values between two slices was used by the slice subtraction method in our previously proposed scheme.[10] In other words, differences of pixel values between a current pixel and the other side pixel, e.g. an anterior side pixel, were not used. In this study, we developed a 3D difference (3DD) filter using 17 neighboring pixel values for the extraction of low-intensity regions.

Figure 4 illustrates the 3DD filter mask. The 3DD filter was defined as the difference pixel values between the current pixel value $f(x,y,z)$ and the mean pixel value of 17 neighboring pixels. The 3DD filter value $g(x,y,z)$ was given by

$$g(x,y,z) = \max_{l} \frac{1}{17} \left\{ \sum_{k} \sum_{j} \sum_{i} f(x+i, y+j, z+k) - f(x,y,z) \right\} - f(x,y,z)$$
$$\begin{pmatrix} i & = & -r, 0, r \\ j & = & -r, 0 \\ k & = & -l, 0, l \\ r & = & ld/\delta \\ l & = & 1, \cdots, R/d \end{pmatrix}, \tag{1}$$

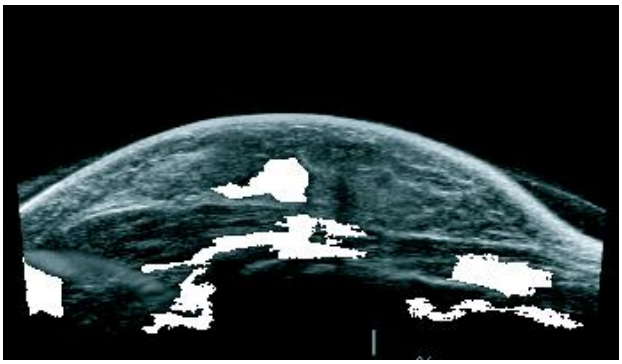

Figure 5. Example of the computerized extraction of low-intensity regions for the image shown in Fig. 2.

where δ and d are the pixel size and the slice interval of the whole breast US image, respectively, and R is the maximum radius of mass to detect. Neighboring pixels on the posterior side of the current pixel, i.e. $f(x+i, y+r, z+k)$, were not used in order to eliminate the effect of posterior echo attenuation. The difference pixel values were calculated in each slice number l and the maximum value was defined as the 3DD filter value.

Finally, low-intensity regions were extracted by using a region growing algorithm based on the 3DD filter value. Seed regions were defined as

$$g(x, y, z) \geq 40, \tag{2}$$

and

$$f(x, y, z) \leq 190. \tag{3}$$

The criterion for region growing was defined as

$$g(x, y, z) \geq 20, \tag{4}$$

and

$$\mu - \sigma \leq f(x, y, z) \leq \mu + \sigma, \tag{5}$$

where μ and σ are the mean pixel value and the standard deviation of pixel values in a seed region, respectively. These threshold values were selected empirically. Figure 5 shows an example of extracted low-intensity regions.

3.3 Initial detection of mass candidates

An area of a segmented region (SR) obtained in the third step (Segmentation of mass candidates) is denoted by ASR. If the area of a low-intensity region included in the SR was greater than or equal to 65% of the ASR, the SR was detected as an initial mass candidate region.

3.4 Feature extraction

In this study, in addition to the previous five features (area, average density, position of center of gravity, difference of average density, and depth-to-width), other five features, i.e., roundness, standard deviation of pixel values, posterior shadowing feature (PSF), and the maximum and the mean of 3DD filter values were extracted. The PSF was defined as

$$PSF = I_{post} - I_{left,right}, \tag{6}$$

where I_{post} and $I_{left,right}$ are the mean pixel value of the posterior region of a mass candidate region and the posterior left and right regions of the mass candidate region, respectively, as illustrated in Figure 6. In order to exclude the bilateral posterior shadowing artifacts, the posterior region was defined only posterior to the central $3w/4$ portion of the mass candidate region, where w is the width of the mass candidate region.

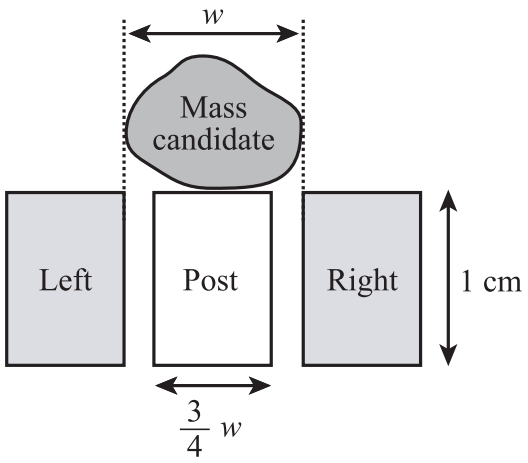

Figure 6. The definition of the posterior shadowing feature (PSF). PSF was defined as the difference value between the mean pixel value of the posterior region of a mass candidate region "Post" and the mean pixel value of "Left" and "Right" regions. w is the width of a mass candidate region.

3.5 False-positive reduction

FPs were reduced employing rule-based technique and QDA analysis using the 10 features described above. The quadratic discriminant function is given as

$$h(\boldsymbol{X}) = \frac{1}{2}(\boldsymbol{X}-\boldsymbol{M}_L)^T\boldsymbol{\Sigma}_L^{-1}(\boldsymbol{X}-\boldsymbol{M}_L) - \frac{1}{2}(\boldsymbol{X}-\boldsymbol{M}_F)^T\boldsymbol{\Sigma}_F^{-1}(\boldsymbol{X}-\boldsymbol{M}_F) + \frac{1}{2}\log\frac{|\boldsymbol{\Sigma}_L|}{|\boldsymbol{\Sigma}_F|}, \tag{7}$$

where $\boldsymbol{X}$ is a feature vector of all candidates. $(\boldsymbol{M}_L, \boldsymbol{\Sigma}_L)$ and $(\boldsymbol{M}_F, \boldsymbol{\Sigma}_F)$ are the mean feature vectors and covariance matrix of the features in the mass candidates and the FPs, respectively.

4. RESULTS AND DISCUSSION

Figure 7 shows an example of the computerized detection of a mass by use of our improved CAD scheme. The performance of our previous and improved CAD schemes for the detection of masses indicated that their sensitivities in detecting masses were 80.0% (56/70) at the level of 16.8 FPs (4379/260) per breast and 80.0% (56/70) at the level of 9.5 FPs (2470/260) per breast, respectively. The FPs of the improved method were reduced by 44% as compared to the previous method. Figure 8 illustrates the FROC curves for the previous and the improved CAD schemes, where the FROC curve for the improved scheme is also superior to the other curve. Therefore, it is clear that low-intensity regions were efficiently extracted from breast US images by use of the 3DD filter.

However, a large number of FPs still remained even after applying the reduction procedure for FPs. These remaining FPs corresponded to the fat and rib regions. It was also difficult to detect a mass with indistinct margin because near-vertical edges as a cue to identify mass candidates were not detected.

5. CONCLUSION

We developed a 3DD filter for the extraction of low-intensity regions and features for the reduction of FPs. The low-intensity regions extracted using the 3DD filter were useful for the detection of mass candidate regions and the extracted features based on the 3DD filter value were effective in reducing the FPs; the FPs were reduced by 44% as compared to the previous method. In the future work, we still need to improve our CAD scheme for a further reduction of FPs.

Figure 7. Example of the computerized detection of a mass for the image shown in Figure 2.

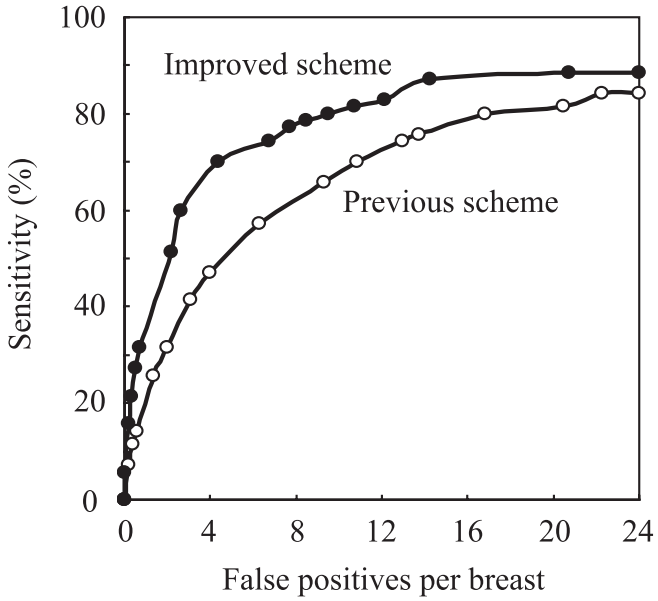

Figure 8. FROC curves for our previous and improved CAD schemes for the detection of masses in whole breast ultrasound images.

ACKNOWLEDGMENTS

This work is supported in part by a grant for the Knowledge Cluster Gifu-Ogaki from Ministry of Education, Culture, Sports, Science and Technology, Japan. The authors are grateful to ALOKA CO., LTD., Japan and TAK CO., LTD., Japan for their assistance in this study. The authors would like to thank the members of Fujita Laboratory in Graduate School of Medicine, Gifu University, Japan for their helpful comments and discussions.

REFERENCES

1. H. M. Zonderland, E. G. Coerkamp, M. J. V. de Vijver, and A. E. V. Voorthuisen, "Diagnosis of breast cancer: Contribution of us as an adjunct to mammography," *Radiology* **213**, pp. 413–422, 1999.
2. M. S. Soo, E. L. Rosen, J. A. Baker, T. T. Vo, and B. A. Boyd, "Negative predictive value of sonography with mammography in patients with palpable breast lesions," *Am. J. Roentgenol* **177**, pp. 1167–1170, 2001.
3. Y. H. Chou, C. M. Tiu, J. Chen, and R. F. Chang, "Automated full-field breast ultrasonography: The past and the present," *J. Med. Ultrasound* **15**, pp. 31–44, 2007.

4. E. Takada, Y. Ikedo, D. Fukuoka, T. Hara, H. Fujita, T. Endo, and T. Morita, "Semi-automatic ultrasonic full-breast scanner and computer-assisted detection system for breast cancer mass screening," in *Medical Imaging 2007: Ultrasonic Imaging and Signal Processing*, S. Y. Emelianov and S. A. McAleavey, eds., *Proc. of SPIE* **6513**, pp. 651310–1–651310–8, 2007.
5. K. Drukker, M. L. Giger, K. Horsch, M. A. Kupinski, and C. J. Vyborny, "Computerized lesion detection on breast ultrasound," *Med. Phys.* **29**, pp. 1438–1446, 2002.
6. K. Drukker, M. L. Giger, C. J. Vyborny, and E. B. Mendelson, "Computerized detection and classification of cancer on breast ultrasound," *Acad. Radiol.* **11**, pp. 526–535, 2004.
7. R. F. Chang, C. J. Chen, E. Takada, C. M. Kuo, and D. R. Chen, "Image stitching and computer-aided diagnosis for whole breast ultrasound image," in *International Journal of Computer Assisted Radiology and Surgery*, H. U. Lemke, K. Inamrua, K. Doi, M. W. Vannier, and A. G. Farman, eds., *Proc. of the 20th International Congress and Exhibition* **1**, pp. 340–343, 2006.
8. D. Fukuoka, T. Hara, H. Fujita, T. Endo, and Y. Kato, "Automated detection and classification of masses on breast ultrasonograms and its 3D imaging technique," in *5th International Workshop on Digital Mammography*, M. J. Yaffe, ed., *Proc. of IWDM 2000*, pp. 182–188, 2001.
9. Y. Ikedo, D. Fukuoka, T. Hara, H. Fujita, E. Takada, T. Endo, and T. Morita, "Computer-aided detection system of breast masses on ultrasound images," in *SPIE Medical Imaging 2006: Image Processing*, J. M. Reinhardt and J. P. W. Pluim, eds., *Proc. of SPIE* **6144**, pp. 61445L1–61445L8, 2006.
10. Y. Ikedo, D. Fukuoka, T. Hara, H. Fujita, E. Takada, T. Endo, and T. Morita, "Development of a fully automatic scheme for detection of masses in whole breast ultrasound images," *Med. Phys.* **34**, pp. 4378–4388, 2007.
11. P. Perona and J. Malik, "Scale-space and edge detection using anisotropic diffusion," *IEEE Trans. Pattern Anal. Mach. Intell.* **12**, pp. 629–639, 1990.
12. J. F. Canny, "A computational approach to edge detection," *IEEE Trans. Pattern Anal. Mach. Intell.* **8**, pp. 679–698, 1986.
13. Y. L. Huang and D. R. Chen, "Watershed segmentation for breast tumor in 2-d sonography," *Ultrasound in Medicine & Biology* **30**, pp. 625–632, 2004.
14. L. Vincent and P. Soille, "Watersheds in digital spaces: An efficient algorithm based on immersion simulations," *IEEE Trans. Pattern Anal. Mach. Intell.* **13**, pp. 583–598, 1991.